JOURNAL OF CATALYSIS **158,** 64–75 (1996)
ARTICLE NO. 0006

Reforming of Methane with Carbon Dioxide to Synthesis Gas over Supported Rhodium Catalysts

II. A Steady-State Tracing Analysis: Mechanistic Aspects of the Carbon and Oxygen Reaction Pathways to Form CO

A. M. Efstathiou, A. Kladi, V. A. Tsipouriari, and X. E. Verykios

Institute of Chemical Engineering and High Temperature Chemical Processes, Department of Chemical Engineering, University of Patras, P.O. Box 1414, Patras GR-26500, Greece

Received September 1, 1994; revised May 3, 1995; accepted August 25, 1995

Steady-state tracing techniques have been applied to investigate mechanistic aspects of the CH_4 reforming reaction over CO_2 over Rh supported on yttria-stabilized zirconia (YSZ) and Al_2O_3 as catalysts. It was found that the surface coverage of active carbon-containing species, which are found in the reaction pathway to CO formation, is of the order of 0.2 over the Rh/Al_2O_3 catalyst, while it is very small ($\theta_c < 0.02$) over Rh/YSZ. The surface coverage of active oxygen-containing species which lead to the formation of CO is found to be very small over both Rh/Al_2O_3 and Rh/YSZ catalysts. However, over the Rh/YSZ catalyst it was found that there exists a large reservoir of lattice oxygen species of the carrier which interact reversibly with gaseous CO_2 under reforming reaction conditions. A spillover of these lattice oxygen species onto the Rh surface seems to occur, contributing to the formation of CO and H_2O. This reaction route proceeds in parallel with the reforming reaction on the Rh surface.

INTRODUCTION

The background to the present study, and reference to previous relevant literature, is given in Part 1 of this work (1). In that paper, the effects of carrier and average metal particle size on the catalytic performance of Rh under conditions of reforming of CH_4 with CO_2 were discussed (1). In particular, emphasis was given to the effects of the carrier and of Rh particle size on the intrinsic initial specific activity and deactivation characteristics of the catalysts. Various H_2 chemisorption experiments, combined with the TPD technique, allowed us to investigate possible causes of catalyst deactivation. The highest initial specific activity was obtained when Rh was supported on yttria-stabilized zirconia (YSZ) followed by γ-Al_2O_3 among the carriers investigated, namely, YSZ, γ-Al_2O_3, TiO_2, SiO_2, La_2O_3, and MgO.

In order to obtain further information concerning the differences in specific activity and deactivation characteristics between the Rh/YSZ and the Rh/Al_2O_3 catalysts and also to explore the mechanism of the present reaction system, the steady-state tracing technique (using isotopically labelled molecules $^{13}CH_4$, $^{13}CO_2$, and $C^{18}O_2$) and other transient methods have been applied in the present work. The surface coverages of active carbon- and oxygen-containing surface intermediate species have been measured under integral reactor conditions. The relatively high activity of the catalysts used did not allow quantification of the coverage of intermediate species under differential reaction conditions. It is suggested through the steady-state tracing technique that a spillover mechanism of oxygen species from the YSZ support onto the Rh surface may contribute to the formation of CO and H_2O under reaction conditions. This reaction route proceeds in parallel with the direct supply of oxygen species onto the Rh surface via dissociation of CO_2 and CO.

To our knowledge, the present work provides for the first time steady-state tracing experimental results on the reforming reaction of CH_4 with CO_2, and also probes the origin of the carbon species (CH_4 or CO_2 molecule) accumulated on the surface of supported Rh catalysts.

EXPERIMENTAL

(*a*) *Catalysts Reactor and Flow System*

The preparation and characterization methods of the present Rh/Al_2O_3 and Rh/YSZ catalysts, as well as the flow system used in transient studies, have already been described in Part 1 of this work (1) and elsewhere (2). The reactor used in the present work consists of two 4.0 mm i.d. sections of quartz tubes which serve as inlet and outlet to and from a quartz cell of 7.0 mm i.d. (nominal volume

0021-9517/96 $12.00

2 ml). The entrance to the reactor cell was machined in such a way as to create local gas mixing. The behavior of the entire reactor cell at the flow rate of 30 ml/min (ambient) is close to that of a single CSTR, as evidenced by the Ar response signal, following the switch He → Ar/He, and the analysis presented elsewhere (3, 4). Heating was provided by a small furnace controlled by a programmable temperature controller. The temperature of the catalyst was measured by a K-type thermocouple placed within a quartz capillary well in the middle of the catalyst bed. Certain details which apply particularly to the experiments involving isotopes (steady-state tracing technique) are reported here.

(*b*) *Isotopic Mixtures*

A mixture consisting of 20% $^{13}CH_4$, 20% CO_2, and 60% He was prepared using a lecture bottle of $^{13}CH_4$ which was of 99% ^{13}C content (Isotec Inc., USA). A mixture consisting of 20% CH_4, 15% CO_2, 5% $C^{18}O_2$, and 60% He was also prepared. To save isotopically labelled gas $C^{18}O_2$, and to reduce the contribution of $C^{18}O_2$ to the $C^{18}O$ signal due to cracking in the mass spectrometer, not all the 20% CO_2 in the ordinary mixture was replaced by $C^{18}O_2$ but only 5%. The $C^{18}O_2$ was of 96.3% ^{18}O purity (L'Air-Liquide, France). Similarly, the $CH_4/^{13}CO_2$/He mixture consisted of 20% CH_4, 15% CO_2, 5% $^{13}CO_2$, and 60% He. The $^{13}CO_2$ was of 99% ^{13}C content (L'Air-Liquide, France). One percent Ar was also added to all isotopic mixtures (replacing 1% of He gas) to facilitate obtaining the response curve of the gas not adsorbing or reacting with the catalyst. This response, when compared to the Ar response obtained upon bypassing the reactor, can be used to determine the hold-up of gas in the reactor (3, 4). All gas mixtures were used at the flow rate of 30 ml/min (ambient).

(*c*) *Mass Spectrometry*

Chemical analysis of the gases during transients was done by an on-line mass spectrometer (Fisons, SXP Elite 300H) equipped with a fast response inlet capillary system. For the steady-state tracing experiments, 20 points/s could be recorded for a given peak (no scanning of the mass scale) using the electron multiplier detector. In the multiple peak data acquisition mode, 4 peaks/s could be followed with good signal to noise ratio. Calibration of the mass spectrometer signal was performed based on prepared mixtures of known compositions. The output signal from the mass spectrometer detector was then converted to mole fraction, y (mol%), by appropriate software.

In the steady-state tracing experiments, the measurement of the responses of $^{13}CH_4$, $^{13}CO_2$, ^{13}CO, and $C^{18}O$, which allow quantification of active carbon-containing and oxygen-containing intermediate species in the reaction pathways from CH_4 and CO_2 to CO, was performed by recording the signals at m/z = 17, 45, 29, and 30, respectively. For the measurement of ^{13}CO (m/z = 29) in the presence of $^{13}CO_2$ (m/z = 45), the contribution of the $^{13}CO_2$ to the 29 peak was estimated by feeding to the mass spectrometer a mixture containing a given concentration of $^{13}CO_2$ in He. During this experiment, the settings in the ion source of the mass spectrometer were the same as those used in the real steady-state tracing experiments. Similar measurements were performed to estimate the ratio of 30/48 for the contribution of $C^{18}O_2$ (m/z = 48) to the m/z = 30 ($C^{18}O$). In other transient experiments, the gases H_2, CH_4, H_2O, $H_2{}^{18}O$, C_2H_6, $^{16}O^{18}O$, $^{18}O_2$, and $C^{16}O^{18}O$ were recorded at m/z = 2, 15, 18, 20, 30, 34, 36, and 46, respectively.

(*d*) *FTIR Spectroscopy*

A Nicolet 740 FTIR spectrometer equipped with a DRIFT cell was used in the present study. The cell, containing ZnSe windows which were cooled by circulating water through blocks in thermal contact with the windows, allowed *in situ* collection of spectra in the temperature range 20–650°C and 1 atm pressure. For all spectra recorded, a 32-scan data acquisition was carried out at a resolution of 4.0 cm^{-1}. During measurements, external optics were purged with dry nitrogen in order to minimize the level of water vapor and carbon dioxide in the IR cell. The sample used (~50 mg) was in finely powdered form and its surface was carefully flattened in order to increase the intensity of the IR beam by reflection. Before exposure to the CH_4/CO_2/He mixture, the catalyst sample was heated in He to 500°C and then the feed was changed to H_2 for 1 h for reduction. The sample was subsequently exposed to He at the reaction temperature to purge the reactor from H_2 and also to collect a background spectrum, before switching to the reaction mixture.

RESULTS

(*a*) *Steady-State Tracing*

Figure 1 shows the response of the reactor outlet composition after the switch CH_4/CO_2/He (2 h) → $CH_4/^{13}CO_2$/He/Ar (5 min) → CH_4/CO_2/He(t) at 650°C is made over the 0.5 wt% Rh/Al_2O_3 catalyst. Here, t designates the real time of the experiment. The results are expressed in terms of the variable Z, which represents the fraction of the ultimate change (giving Z = 1) as a function of time. Thus, Z is defined by

$$Z(t) = (y(t) - y_\infty)/(y_o - y_\infty), \qquad [1]$$

where the subscripts o and ∞ refer to values of y (mole fraction) just before the switch (t = 0) and long after the switch ($t \to \infty$). Therefore, Z varies from 1 (t = 0) to 0

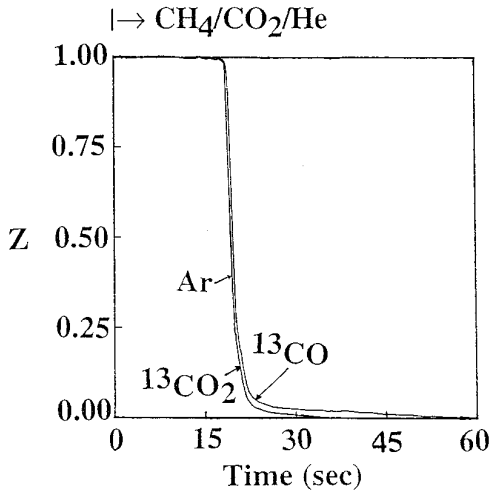

FIG. 1. Steady-state tracing of the reforming reaction of CH_4 with CO_2 at 650°C over the Rh/Al_2O_3 catalyst. Gas delivery sequence: CH_4/CO_2/He (650°C, 2 h) → $CH_4/^{13}CO_2$/He/Ar (650°C, 5 min) → CH_4/CO_2/He (650°C, t). The transient responses of Ar, ^{13}CO, and $^{13}CO_2$ are shown. Amount of sample used $W = 0.25$ g; $Q = 30$ ml/min (ambient).

($t \to \infty$). The curve labelled as Ar is the argon response as the gas passes through the reactor containing the catalyst sample. For the curve labelled $^{13}CO_2$, y represents the mole fraction of $^{13}CO_2$ in the gas phase at the reactor outlet. Thus, if there were no reversibly adsorbed $^{12}CO_2$ under $^{12}CH_4/^{12}CO_2$/He treatment, then the $^{13}CO_2$ response would have been identical to the Ar response curve. This is indeed what is observed, as indicated in Fig. 1, which shows the Ar and $^{13}CO_2$ curves to be exactly superimposed. On the other hand, the ^{13}CO response curve is above the Ar curve at all times during the transient, a result which indicates that there is an amount of active carbon-containing intermediate species on the catalyst surface (i.e., CH_x) which are found in the carbon pathway from CO_2 to form CO.

The ^{13}CO response which is shown in Fig. 1 reflects the transient incorporation of ^{12}C into a ^{13}C carbon-containing intermediate species pool, which eventually leads to a steady-state ^{12}CO production rate. In other words, the decay of the ^{13}CO response curve represents the depletion of ^{13}C-containing intermediate species pool(s). The area difference between the ^{13}CO and Ar curves is proportional to the amount of carbon-containing intermediate species which are in the carbon-pathway to form CO. This amount is found to be 2.5 μmol/g, which corresponds to θ_c of 0.2 (based on 25% Rh dispersion (1)). At the conditions of the experiment shown in Fig. 1, the CH_4 conversion is 60% and the CO_2 conversion is 65%. Similar experiments at CH_4 conversions less than 15% (amount of catalyst used less than 10 mg) did not allow an accurate measurement of active carbon because of its small quantity, as is evidenced by the closeness of the Ar and ^{13}CO response curves shown in Fig. 1. Another experimental difficulty of accurately quantifying the ^{13}CO response at low CH_4, and, therefore, CO_2 conversions, is the contribution of the inherently high $^{13}CO_2^+$ ($m/z = 45$) signal to the signal of $^{13}CO^+$ ($m/z = 29$) due to cracking in the source of the mass spectrometer under the conditions of the present experiment.

A steady-state tracing experiment (labelling the feed with $^{13}CH_4$) similar to that presented in Fig. 1 was conducted using the sequence: CH_4/CO_2/He (650°C, 2 h) → $^{13}CH_4/CO_2$/He/Ar (650°C, 5 min) → CH_4/CO_2/He (650°C, t). The $^{13}CH_4$, ^{13}CO, and Ar responses obtained under the last CH_4/CO_2/He treatment of the above described gas delivery sequence were identical, indicating that practically neither reversibly adsorbed CH_4 nor active carbon, produced from methane, accumulate on the catalyst surface under reaction conditions.

In order to estimate the oxygen reservoir present on the catalyst surface which participates in the production of CO, a similar steady-state tracing experiment to that described in Fig. 1 was performed using $C^{18}O_2$ in the feed stream. Thus, the following sequence was applied: CH_4/CO_2/He (650°C, 2 h) → $CH_4/C^{18}O_2$/He/Ar (650°C, 5 min) → CH_4/CO_2/He (650°C, t). Here, the $C^{18}O$ and Ar responses were of interest. These responses, measured during the last switch of the sequence described above were found to be identical, indicating that under the reaction conditions investigated, the amount of active oxygen species on the catalyst surface is practically immeasurable. It is noted here that from the present steady-state tracing technique and the reaction system investigated, surface coverages of less than 2% cannot be measured (see also the relative position of Ar and ^{13}CO response curves shown in Fig. 1).

The formation of H_2O (by-product of the present reforming reaction) also involves the participation of oxygen-containing adsorbed species on the catalyst surface. Attempts were made to measure the pool of active oxygen species which are in the oxygen-pathway of water formation. The same steady-state tracing experiment as that described in the previous paragraph (using $C^{18}O_2$ in the feed) was performed, while the decay response of $H_2{}^{18}O$ during the switch $CH_4/C^{18}O_2$/He/Ar → CH_4/CO_2/He(t) was of interest. The $H_2{}^{18}O$ response which was obtained was not compared to the Ar response in this case (due to adsorption/desorption of water in the lines and the mass spectrometer), but with the H_2O response obtained in the case of purging gaseous H_2O from the reactor. The latter response was obtained following the switch H_2O/He → He(t) at 650°C, in the absence of catalyst sample (replaced by quartz chips), and for a similar H_2O concentration as that obtained in the reforming reaction (Fig. 1). This blank experiment dictates the H_2O response from the switching

valve, through the reactor, to the mass spectrometer detector. It is noted here that the pathway of gas travelling from the switching valve to the inlet of the reactor is small compared to that from the outlet of the reactor to the detector. In other words, the response characteristics of the hydrodynamics of the system are much influenced by the reactor volume and the lines after the reactor. When this H_2O response (in its dimensionless form, Z vs time) was compared to the response of $H_2{}^{18}O$ obtained during steady-state tracing, it was found that practically both responses were identical.

Figure 2 shows gas-phase dimensionless transient responses of Ar, ^{13}CO, and $^{13}CO_2$ following the sequence: $CH_4/CO_2/He$ (650°C, 2 h) → $CH_4/^{13}CO_2/Ar/He$ (650°C, 5 min) → $CH_4/CO_2/He$ (650°C, t) obtained over the 0.5 wt% Rh/YSZ catalyst. As is shown in Fig. 2, both the $^{13}CO_2$ and ^{13}CO response curves overlap with the response curve of Ar, indicating that neither reversibly adsorbed CO_2 nor carbon-containing species derived from CO_2 and leading to CO accumulate on the catalyst surface under the present experimental conditions. A similar steady-state tracing experiment as that described above, but using $^{13}CH_4$ in the feed stream and following the responses of Ar, ^{13}CO, and $^{13}CH_4$, resulted again in an overlap of both $^{13}CH_4$ and ^{13}CO response curves with the Ar response curve. These results indicate that neither reversibly adsorbed CH_4 nor carbon-containing intermediate species derived from the CH_4 molecule and leading to CO accumulate on the catalyst surface under the present reforming reaction conditions.

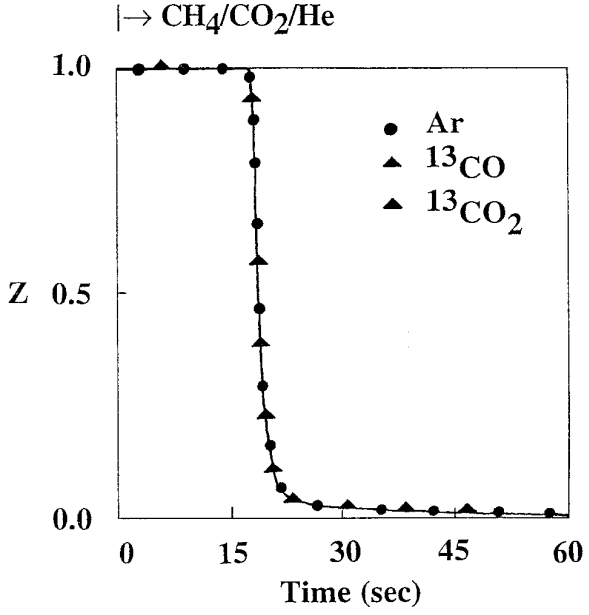

FIG. 2. Steady-state tracing of the reforming reaction of CH_4 with CO_2 at 650°C over the Rh/YSZ catalyst. Gas delivery sequence: $CH_4/CO_2/He$ (650°C, 2 h) → $CH_4/^{13}CO_2/He/Ar$ (650°C, 5 min) → $CH_4/CO_2/He$ (650°C, t). The transient responses of Ar, ^{13}CO, and $^{13}CO_2$ are shown. Amount of sample used W = 0.5 g; Q = 30 ml/min (ambient).

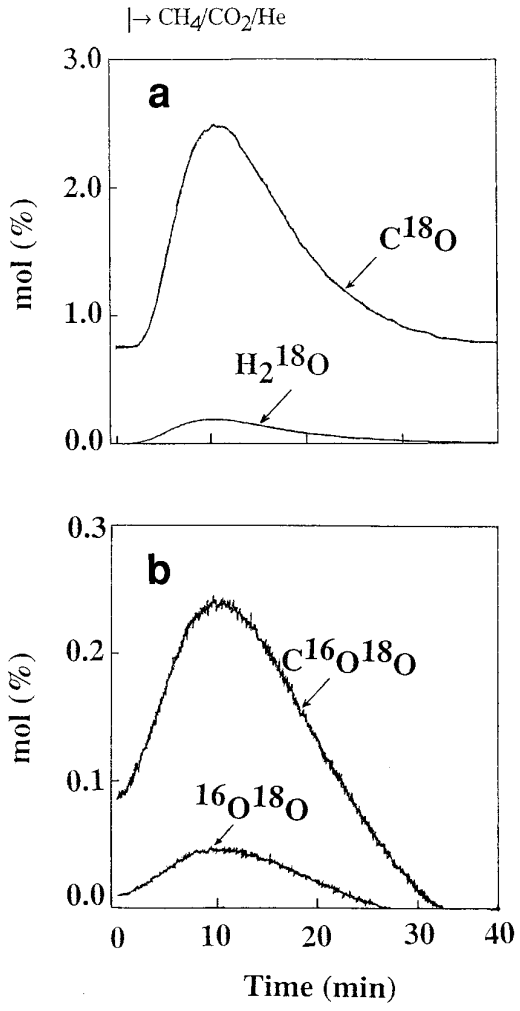

FIG. 3. Steady-state tracing of the reforming reaction of CH_4 with CO_2 at 650°C over the Rh/YSZ catalyst. Gas delivery sequence: $CH_4/CO_2/He$ (650°C, 2 h) → $CH_4/C^{18}O_2/He/Ar$ (650°C, 5 min) → $CH_4/CO_2/He$ (650°C, t). The transient responses of (a) $C^{18}O$ and $H_2{}^{18}O$ and (b) $C^{16}O^{18}O$ and $^{16}O^{18}O$ are shown. Amount of sample used W = 0.5 g; Q = 30 ml/min (ambient).

The oxygen-pathway of the reforming reaction of CH_4 with CO_2 at 650°C over the Rh/YSZ catalyst was investigated by applying the steady-state tracing technique (using $C^{18}O_2$) in a similar manner as reported previously for the Rh/Al_2O_3 catalyst. Figures 3a and 3b show transient responses (mol% vs time) of gaseous $C^{18}O$, $H_2{}^{18}O$, $C^{16}O^{18}O$, and $^{16}O^{18}O$ obtained under the last $CH_4/CO_2/He$ switch of the following delivery sequence: $CH_4/CO_2/He$ (650°C, 2 h) → $CH_4/C^{18}O_2/Ar/He$ (650°C, 5 min) → $CH_4/CO_2/He$ (650°C, t). In Fig. 3a, the $C^{18}O$ response remains constant for approximately 2 min after the switch of the feed from $CH_4/C^{18}O_2/Ar/He$ to $CH_4/CO_2/He$, while it goes through

a maximum after 10 min on stream in CH_4/CO_2/He mixture. This transient lasts for more than 40 min, as Fig. 3a indicates. Similar transient response curves were obtained for $H_2{}^{18}O$, $C^{16}O^{18}O$, and $^{16}O^{18}O$ (Figs. 3a and 3b). It is noted that only a small response of $C^{18}O_2$ was obtained during the switch corresponding to the results shown in Fig. 3. The transient responses of gaseous species containing ^{18}O shown in Fig. 3 clearly suggest that, during the 5-min treatment of the Rh/YSZ catalyst at 650°C with $CH_4/C^{18}O_2$/He, a large reservoir of ^{18}O species is formed which subsequently is depleted under CH_4/CO_2/He treatment through reactions leading to $C^{18}O$, $H_2{}^{18}O$, $^{16}O^{18}O$, and $C^{16}O^{18}O$. Integration of all responses shown in Fig. 3 for the period of 40 min under the CH_4/CO_2/He treatment provides an amount of 1500 μmol/g_{cat} of oxygen species. This number corresponds to 75 monolayers of exposed Rh atoms (assuming $O_s/Rh_s = 1$). This result clearly indicates that the corresponding quantity of oxygen species accumulated on the catalyst surface during $CH_4/C^{18}O_2$/He treatment cannot reside on the Rh surface but must be on the yttria-stabilized zirconia support. To further explore this view, various other transient isotopic experiments over the YSZ support alone have been conducted, and these are described below.

(*b*) *Transient Isotopic Experiments over Yttria-Stabilized Zirconia*

Yttria stabilized zirconia (YSZ) is known to be one of the best oxygen ion conductors among solid electrolytes (5). Oxygen anion species are, therefore, the major ionic charge-carriers in this material. In the present work, of particular interest are the exchange properties of these oxygen species with respect to gaseous oxygen, and, most importantly, with respect to carbon dioxide under reforming reaction conditions.

Figure 4 shows transient responses of gaseous $^{16}O^{18}O$ and $^{18}O_2$ species obtained over pure YSZ (0.3 g) following the switch He → 1% $^{18}O_2$/He(t) at 650°C. Before this switch was applied, the catalyst was treated at 500°C with 10% O_2/He for 5 h. There is a clear production of $^{16}O^{18}O$ and consumption of $^{18}O_2$ gases indicating that exchange reactions of gaseous $^{18}O_2$ with the lattice oxygen species of YSZ occur at the conditions of the experiment. After about 1 min of $^{18}O_2$/He treatment, a pseudo-steady-state rate of $^{16}O^{18}O$ production is obtained, and this is calculated to be 0.26 μmol/m^2 min. An ^{18}O material balance over a period of 2.5 min results in a 17.3 μmol ^{18}O/g accumulated within the lattice of YSZ (40 ml/min $^{18}O_2$/He flow).

The exchange reaction of lattice oxygen of pure YSZ with the oxygen of the CO_2 molecule was investigated as follows: The YSZ carrier was first treated with 1% $^{18}O_2$/He mixture at 650°C for 10 min (to replace some amount of its lattice ^{16}O species with ^{18}O, see Fig. 4). The feed was

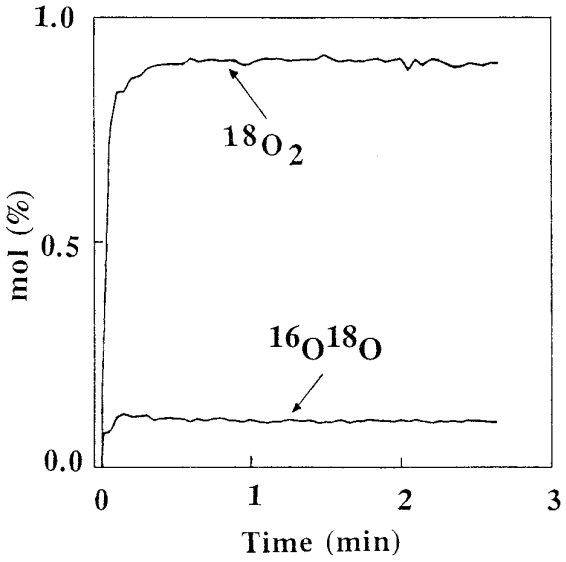

FIG. 4. Transient isotopic responses of $^{18}O_2$ and $^{16}O^{18}O$ obtained at 650°C over the YSZ carrier according to the gas delivery sequence: He → 1% $^{18}O_2$/He (650°C, t). Amount of sample used W = 0.3 g; Q = 40 ml/min (ambient).

then changed to pure He for 3 min in order to purge the gas phase of the reactor and the lines, followed by a switch to the CH_4/CO_2/He feed mixture used for the reforming reaction. Figure 5 shows the transient responses to $C^{16}O^{18}O$ and $^{16}O^{18}O$ obtained during the last switch of the feed stream. It is noted that only small amounts of $C^{18}O_2$ and

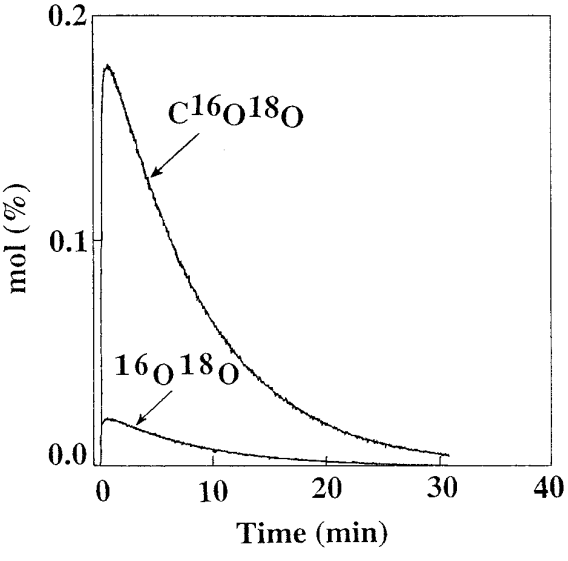

FIG. 5. Transient isotopic responses of $C^{16}O^{18}O$ and $^{16}O^{18}O$ obtained at 650°C over the YSZ carrier according to the gas delivery sequence: 1% $^{18}O_2$/He (650°C, 10 min) → He (650°C, 3 min) → CH_4/CO_2/He (650°C, t). Amount of sample used W = 0.3 g; Q = 30 ml/min (ambient).

no $C^{18}O$ gaseous species were measured. The transient response curves of $C^{16}O^{18}O$ and $^{16}O^{18}O$ of Fig. 5 provide an amount of 75.5 μmol ^{18}O/g, a result which is consistent with the amount of ^{18}O accumulated in the lattice of YSZ, as shown in Fig. 4. The time required for the depletion of the ^{18}O reservoir, mainly by reaction by $C^{16}O_2$, is similar to that obtained with the Rh/YSZ catalyst (Fig. 3).

Figure 6 shows the transient response of gaseous $C^{16}O^{18}O$ obtained under CH_4/CO_2/He treatment following the gas delivery sequence: $CH_4/C^{18}O_2$/He (650°C, 5 min) → He (650°C, 3 min) → CH_4/CO_2/He (650°C, t) over pure YSZ. In this experiment, the pool of ^{18}O species is formed during $CH_4/C^{18}O_2$/He treatment of YSZ via exchange of lattice oxygen, $^{16}O_s$, with the ^{18}O atom of the gaseous $C^{18}O_2$ molecule. Again, the transient result of Fig. 6 clearly probes for the large capacity of lattice oxygen of YSZ which readily exchanges with the oxygen of the CO_2 molecule. The amount of ^{18}O corresponding to the $C^{16}O^{18}O$ response of Fig. 6 is found to be 975 μmol/g.

(*c*) *Surface Species Formed during Reforming Reaction of CH_4 with CO_2 Studied by FTIR Spectroscopy*

In situ FTIR spectroscopy was used to study the chemical nature of intermediate species formed during the reforming reaction in the range 500–650°C over the Rh/Al_2O_3 and Rh/YSZ catalysts. In addition, the reactivity of these species towards hydrogenation, and also during He purge, were particularly studied over the Rh/Al_2O_3 system. Figure 7 shows IR bands in the frequency range 2100–1450 cm^{-1} recorded at 500°C with variable time on stream over the Rh/Al_2O_3 catalyst. The IR bands at 2029 and 1800 cm^{-1} correspond to linear and bridged adsorbed CO species (6–8), respectively, while the IR bands at 1590 cm^{-1} signify formate species (9–11). The results of Fig. 7 show that after 4 min on stream the surface coverage of CO stays constant, while there is a continuous accumulation of formate species on the Al_2O_3 support even after 30 min on stream. No infrared CH bands have been detected in the region 3100–2700 cm^{-1}, corresponding to CH_x adsorbed species, while weak IR bands were observed in the region of 1460 cm^{-1}, the latter corresponding to carbonate ionic species (11, 12).

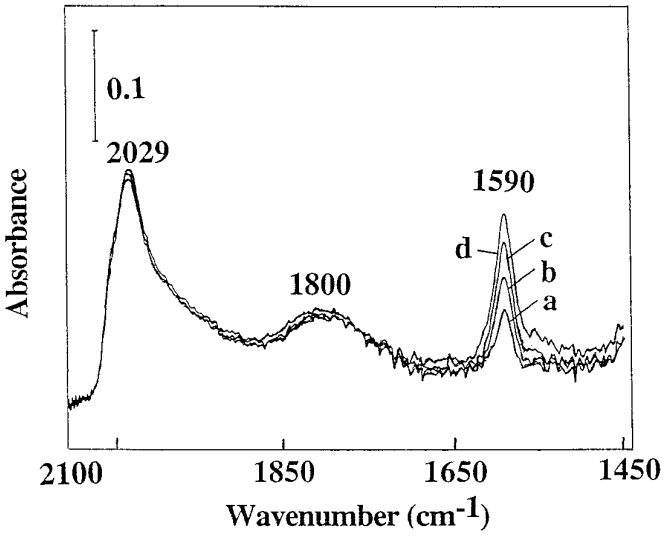

FIG. 7. FTIR spectra in the range 2100–1450 cm^{-1} recorded at 500°C with time on stream, Δt, following the reforming reaction of CH_4 with CO_2 over the Rh/Al_2O_3 catalyst. (a) Δt = 4 min, (b) Δt = 6 min, (c) Δt = 10 min, and (d) Δt = 30 min.

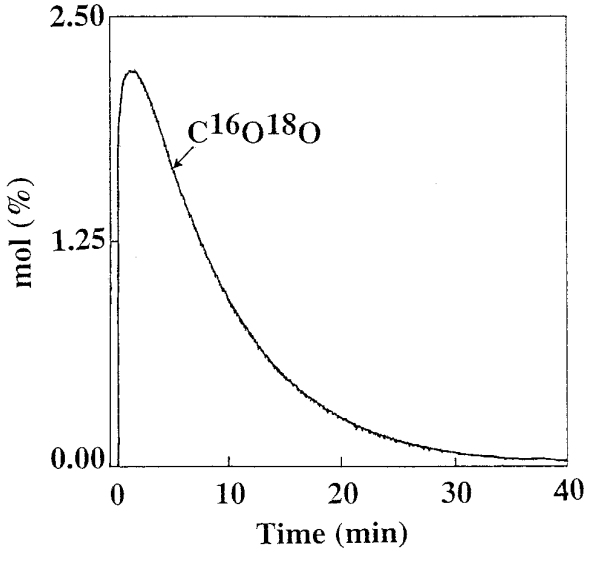

FIG. 6. Transient isotopic response to $C^{16}O^{18}O$ obtained at 650°C over the YSZ carrier according to the gas delivery sequence: $CH_4/C^{18}O_2$/He (650°C, 5 min) → He (650°C, 3 min) → CH_4/CO_2/He (650°C, t). Amount of sample used W = 0.3 g; Q = 30 ml/min (ambient).

By increasing the reaction temperature to 550°C, strong infrared bands in the region of 1460 cm^{-1} were observed, a result not obtained in the case of reaction at 500°C (Fig. 7). On the other hand, formate and adsorbed CO species still accumulated on the surface of the Rh/Al_2O_3 catalyst. Figure 8a shows IR bands in the range of 2100–1300 cm^{-1} recorded at 550°C with variable time on stream, where the development of formate (1589, 1375 cm^{-1}), ionic carbonate, CO_3^{2-} (1456 cm^{-1}), and linear adsorbed CO (2023 cm^{-1}) species are presented. Of interest is the absence of carbonate adsorbed species in the first 5 min of reaction, in contrast to the case of formate species (Fig. 8), and also the absence of bridged CO adsorbed species. It is also noted that the carbonate species (IR band at 1456 cm^{-1}) grow with reaction time even after 30 min on stream in CH_4/CO_2/He mixture.

By increasing the reaction temperature to 650°C, the only adsorbed species on the surface of the Rh/Al_2O_3 catalyst are the linear CO species on the rhodium surface and

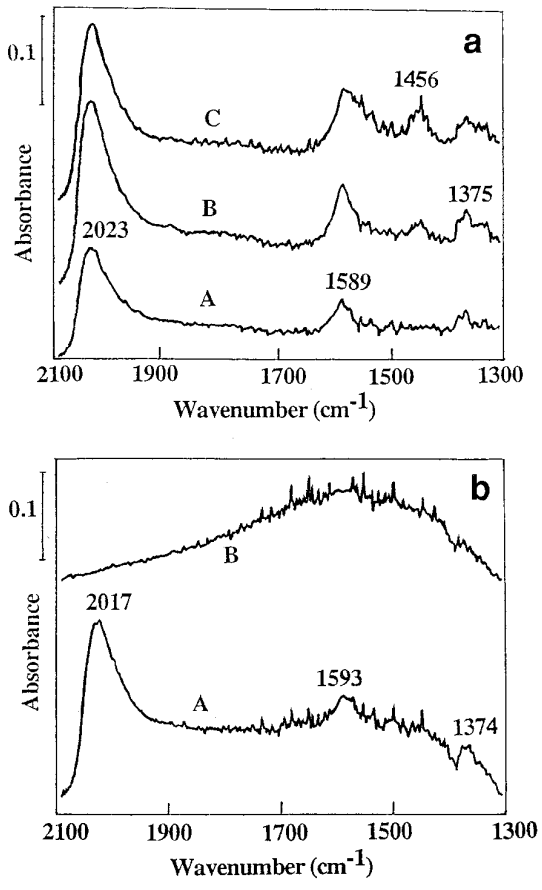

FIG. 8. (a) FTIR spectra in the range 2100–1300 cm^{-1} recorded at 550°C with time on stream, Δt, following the reforming reaction over the Rh/Al_2O_3 catalyst. (A) Δt = 5 min, (B) Δt = 10 min, and (C) Δt = 30 min. (b) FTIR spectra in the range 2100–1300 cm^{-1} recorded at 650°C. (A) Following reforming reaction over the Rh/Al_2O_3 catalyst for 10 min and (B) following a 10-min Ar purge after spectrum (A) was recorded.

the formate species on the alumina surface. Figure 8b, curve (A), shows these results after 10 min of reaction in $CH_4/CO_2/He$ mixture. Curve (B) in Fig. 8b presents the IR spectrum recorded at 650°C following a 10-min Ar purge performed after recording of spectrum shown in (A). It is clearly illustrated that the infrared bands corresponding to both linearly adsorbed CO and formate species entirely disappear after 10 min of Ar purge. As illustrated in the next section, formate species decompose to form CO_2 and H_2, whereas adsorbed CO quickly desorbs into the gas phase at 650°C.

In Part 1 of this work (1), temperature-programmed hydrogenation (TPH) experiments of carbon-containing species formed during the reforming reaction at 650°C resulted in three well-resolved CH_4 peaks in the range 100–450°C. These peaks were assigned to different kinds of carbon species but not to carbonate or formate adsorbed species. Experimental evidence for this assignment is presented in this part of the work via *in situ* FTIR measurements.

Figure 9 shows IR bands in the frequency range 1670–1310 cm^{-1} recorded at different temperatures in 2% H_2/Ar flow following reforming reaction at 550°C for 30 min. Of interest is the reactivity of formate (IR band at 1566 cm^{-1}) and ionic carbonate CO_3^{2-} (IR band at 1458 cm^{-1}) species towards hydrogenation. After reforming reaction, the feed was changed to Ar and the infrared cell was quickly cooled to 200°C in Ar flow. Then, the feed was changed to 2% H_2/Ar mixture, while FTIR spectra were recorded at 200, 300, 400, and 500°C after 10 min of catalyst treatment with 2% H_2Ar. The infrared results shown in Fig. 9 clearly indicate that both formate and carbonate species are stable in H_2/Ar treatment in the range 200–300°C, while only a small decrease in the intensity of the infrared band corresponding to formate species is observed in the range 300–400°C. On the other hand, in the range 400–500°C, both formate and carbonate adsorbed species disappear upon H_2/Ar treatment.

Figure 10 shows IR bands in the frequency range 2100–1450 cm^{-1}, recorded at 500°C, with variable time on stream over the Rh/YSZ catalyst. As in the case of Rh/Al_2O_3 (Fig. 7), the IR band at 2040 cm^{-1} corresponds to linear adsorbed CO species on the Rh surface, while that at 1590 cm^{-1} corresponds to formate species on the YSZ surface. A small shift to higher frequency of the linear CO band is observed on Rh/YSZ as compared to that on Rh/Al_2O_3. On the other hand, an infrared band at 1900 cm^{-1} appears on Rh/YSZ (Fig. 10), not observed on Rh/Al_2O_3, while the IR band corresponding to bridged CO (1800 cm^{-1})

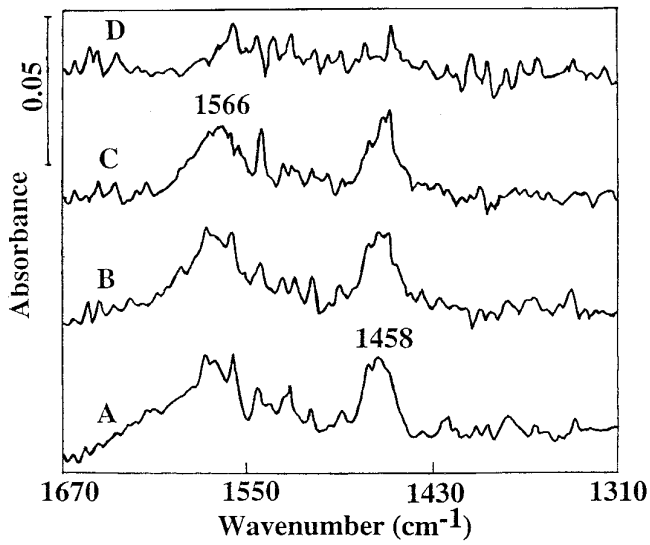

FIG. 9. Stability of infrared bands corresponding to formate (1566 cm^{-1}) and carbonate, CO_3^{2-} (1458 cm^{-1}) species in 2% H_2/Ar flow as a function of temperature. (A) T = 200°C, (B) T = 300°C, (C) T = 400°C, and (D) T = 500°C.

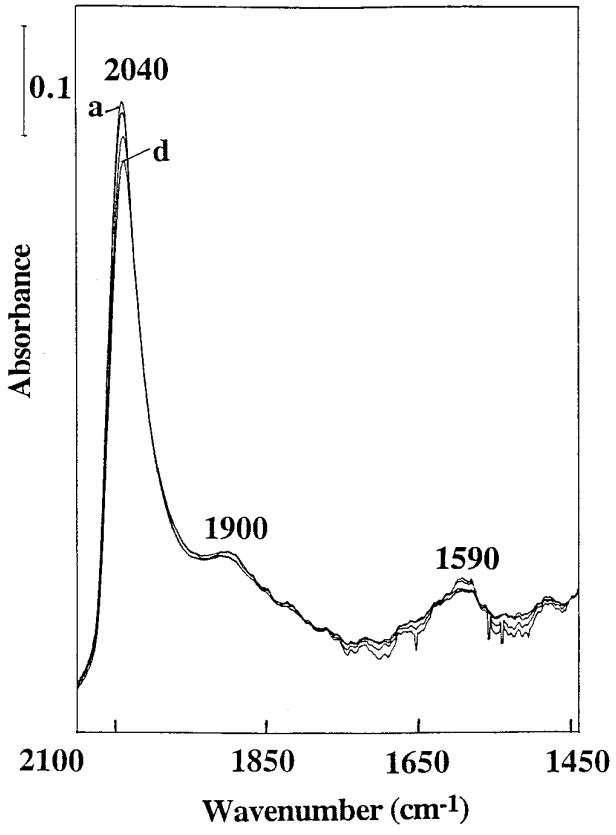

FIG. 10. FTIR spectra in the range 2100–1450 cm^{-1} recorded at 500°C with time on stream, Δt, following reforming reaction of CH_4 with CO_2 over the Rh/YSZ catalyst. (a) Δt = 4 min, (b) Δt = 6 min, (c) Δt = 15 min, and (d) Δt = 30 min.

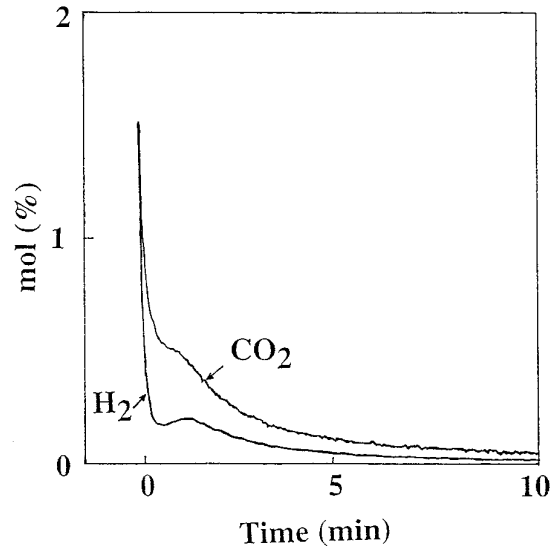

FIG. 11. Transient responses of CO_2 and H_2 obtained at 650°C according to the gas delivery sequence: CH_4/CO_2/He (650°C, 2 h) → He (650°C, t). Amount of the Rh/Al_2O_3 sample used W = 0.25 g; Q = 30 ml/min (ambient).

which appears on Rh/Al_2O_3 (Fig. 7) is not observed over the Rh/YSZ catalyst. The infrared band at 1900 cm^{-1} probably corresponds to a new type of adsorbed CO species, the structure of which is discussed later.

(*d*) *Quantification of Formate Species Formed during Reforming Reaction over the Rh/Al_2O_3 Catalyst*

Mass spectrometry was used to quantify the amount of formate species formed during the reforming reaction at 650°C. It is known that formate species formed over the Al_2O_3 surface decompose in He flow at high temperatures to give mainly CO_2 and H_2 (13). Thus, the experiment conducted was the following. After CH_4/CO_2/He reaction at 650°C for 2 h, the feed was changed to pure He and the H_2 and CO_2 signals were followed with time in He flow. Figure 11 shows transient responses of H_2 and CO_2 produced during He treatment of the catalyst as described above. These responses were recorded after 90 s of the He switch, time sufficient to purge the reactor and the lines. The amounts of H_2 and CO_2 calculated from the transients of Fig. 11 agree very well with the stoichiometry of formate decomposition to H_2 and CO_2 (H_2/CO_2 = 0.5). The amount of formate calculated corresponds to 60 μmol/g (0.6 μmol/m^2) or θ_{HCOO} of 5, based on the Rh exposed surface area. The latter result confirms the previous assignment of formate being located on the Al_2O_3 support. A similar experiment performed over the Rh/YSZ catalyst results in no measurable quantity of formate, a result consistent with the very weak formate infrared bands observed (Fig. 10).

(*e*) *Origin of Carbon Species Accumulated during the Reforming Reaction of CH_4 with CO_2 over the Rh/Al_2O_3 Catalyst*

To investigate the origin of carbon species (CH_4 or CO_2 molecule) formed under reaction conditions over the Rh/Al_2O_3 catalyst, the following experiment was conducted: The catalyst was first treated with $^{13}CH_4/CO_2$/He for 10 min at 650°C followed by a 10-min He purge at 650°C. The reactor was then quickly cooled to 100°C in He flow followed by a switch to O_2/He in order to carry out a temperature-programmed oxidation (TPO) experiment (β = 20°C/min). During this TPO experiment the $^{12}CO_2$ and $^{13}CO_2$ responses were followed by on-line mass spectrometry.

Figure 12 shows the $^{12}CO_2$ and $^{13}CO_2$ responses obtained during the TPO experiment. The $^{12}CO_2$ response is due to the oxidation of carbon species derived from CO_2, while the $^{13}CO_2$ response is due to the oxidation of carbon species derived from the $^{13}CH_4$ molecule during reforming reaction. The sum of the $^{12}CO_2$ and $^{13}CO_2$ responses is in excellent agreement with a similar TPO experiment re-

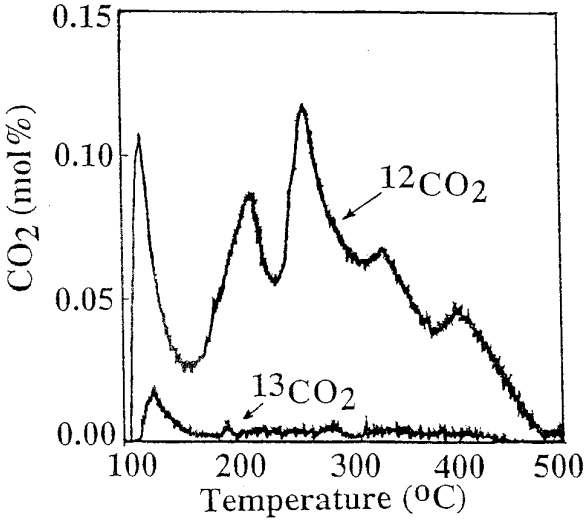

FIG. 12. Transient responses of $^{12}CO_2$ and $^{13}CO_2$ obtained during temperature-programmed oxidation (TPO) of carbon species formed after reforming reaction of CH_4 with CO_2 at 650°C over the Rh/Al_2O_3 catalyst. Gas delivery sequence: $^{13}CH_4/CO_2/He$ (650°C, 10 min) → He (650°C, 10 min) → cool in He flow to 100°C → 10% O_2/He (TPO, β = 20°C/min). Amount of Rh/Al_2O_3 sample used W = 0.5 g; Q = 30 ml/min (ambient).

ported in Part 1 of this work (1) after using the ordinary $CH_4/CO_2/He$ feed mixture. Also note the various $^{12}CO_2$ peaks observed in Fig. 12 which agree in position and amounts to those observed in the TPO experiment reported in Part 1 (1) following $CH_4/CO_2/He$ reaction at 650°C. It becomes clear from the results of Fig. 12 that most of the carbon accumulated over the Rh/Al_2O_3 catalyst is derived from the reaction pathway of CO_2 rather than from the CH_4 molecule.

DISCUSSION

(*a*) *Carbon-Containing Intermediate Species Formed under Reforming Reaction Conditions*

The steady-state tracing technique applied in the present work provides the amount of active carbon-containing species which truly participate in the reaction pathway of CO formation under reforming of CH_4 with CO_2. As explained in the Results Section, this amount corresponds to high CH_4 and CO_2 conversions, and should, therefore, be treated as the result of the effect of a distribution of partial pressures of reactants, developed along the catalyst bed, on the establishment of surface coverages of intermediate species. For a similar CH_4 conversion, the amount of active carbon-containing species formed over the Rh/Al_2O_3 catalyst, which is mainly derived from the CO_2 molecule, corresponds to θ_c of 0.2, while that over the Rh/YSZ catalyst is less than 0.02 of a monolayer. It appears from these results that surface elementary reaction steps of the carbon-pathway of the CO_2 route, which are in sequence and control the rate of CO formation, are slower over Rh/Al_2O_3 than over Rh/YSZ (14). This view, as derived from the steady-state tracing experiments presented in Figs. 1 and 2, is in harmony with the initial TOF values obtained in Part 1 of this work (1) for these two catalysts. In addition, Rh/YSZ also appears to be twice as active as the Rh/Al_2O_3 catalyst after 2 h on stream, as reported elsewhere (15).

The in-situ FTIR results on the reforming reaction at 650°C (Fig. 8b) indicate that there is a measurable quantity of undissociated adsorbed CO species on the Rh surface of the Rh/Al_2O_3 catalyst, whereas the steady-state tracing results of Fig. 1 provided the surface coverage, θ_c, of the active carbon-containing intermediate species from the CO_2 molecular route to form CO. As is discussed in section (b), adsorbed CO intermediate species are present in this reaction route. Therefore, the surface coverage, θ_c, of these active carbon-containing species which lead to the production of CO must include surface adsorbed CO species. Atomic carbon species, bound on the Rh surface, are also considered to be part of this active carbonaceous pool which leads to the formation of CO (θ_c = 0.2, Fig. 1). On the other hand, the amount of formate species (HCOO) present on the Al_2O_3 support (Figs. 7–9, Ref. (16)) is found to exceed the monolayer value (based on the Rh surface) (see Fig. 11). The latter result along with the amount of active carbonaceous species found (θ_c = 0.2) conclusively exclude the possibility that formate species are active intermediate species contributing to the formation of CO under reforming reaction conditions. This species should be considered as a spectator species, as in the case of CO/H_2 reaction over the Rh/Al_2O_3 catalyst (17, 18).

The amount of active carbon species (θ_c = 0.2) formed over the Rh/Al_2O_3 catalyst (Fig. 1) is consistent with the total amount of carbon species accumulated on the catalyst surface, as determined from the TPH and the TPO experiments presented in Part 1 of this work (θ_c = 0.6, Ref. (1)). Thus, inactive carbonaceous species, which do not participate in the reaction mechanism of CO formation, accumulate on the Rh/Al_2O_3 catalyst surface and amount to θ_c of 0.4. Some quantity of these species may reside on the alumina surface.

The amount of active carbon species derived from the CH_4 molecular route and leading to CO is found to be very small ($\theta_c < 0.02$) over both Rh/Al_2O_3 and Rh/YSZ catalysts, a result which suggests that dissociation of CH_4 into CH_x species and oxidation of these species to CO must be considered as fast steps over both catalysts.

The *in situ* FTIR results shown in Figs. 7 and 10 clearly indicate that at 500°C formation of bridged CO species is favored over the Rh/Al_2O_3 but not over the Rh/YSZ catalyst. This may be consistent with the fact that larger Rh particles are obtained over the Rh/Al_2O_3 than Rh/YSZ

catalyst for the same metal loading after reforming reaction conditions (1). It is expected that the rate of desorption of linear CO species would be higher than that of bridged CO species. This result could lead to higher accumulation of carbon, via disproportionation, in the case of bridged as compared to linear CO species under favored reaction conditions. In the present case, accumulation of carbon during reforming reaction at 650°C was observed over the Rh/Al_2O_3 catalyst in much larger quantities than over the Rh/YSZ catalyst (Figs. 1, 2 and Ref. (1)). The latter result may be related to the relative proportion of bridged and linear adsorbed CO species (ratio of their mean life times on the surface) over the two catalysts as discussed above.

The IR band at 1900 cm^{-1} observed during the reforming reaction at 500°C over the Rh/YSZ catalyst (Fig. 10) does not fit the IR spectrum of various CO/Rh organometallic complexes (19). A similar infrared band has been observed by Chuang and Pien (20) over the Rh/SiO_2 catalyst following CO chemisorption, and recently by Efstathiou *et al.* (21) over the Rh/MgO catalyst following CO chemisorption at 250°C. In the latter case, the authors suggested (based on experimental evidence) that the infrared band at 1906 cm^{-1} could be related to the presence of Rh^{n+} oxidized species along the interface formed by the small Rh crystallites and the surface of the MgO support (21). A similar explanation could be offered in the present case of Rh/YSZ catalyst (Fig. 10). Oxidation of rhodium sites at the interface by lattice oxygen of YSZ seems a very likely event in relation to the spillover mechanism of lattice oxygen onto the Rh surface to be discussed next.

The results shown in Fig. 11 indicate that a 10-min He treatment of the catalyst surface at 650°C, following the reforming reaction, is nearly sufficient to decompose all the amount of formate species. The FTIR results shown in Fig. 9 clearly demonstrate that hydrogenation of formate, or its decomposition in H_2/He flow, starts at temperatures at least higher than 300°C. This result agrees very well with the past work of Solymosi *et al.* (9) and a recent transient FTIR work (22) related to the hydrogenation of formate species present on the Al_2O_3 support of a Rh/Al_2O_3 catalyst. It is, therefore, unlikely that the second major CH_4 peak in the TPH spectrum reported in Part 1 of this work (1) corresponds to formate species. Only the very small CH_4 peak observed at $T > 350$°C could partly be attributed to formate species (1).

(*b*) *Mechanistic Aspects of the Reaction of CH_4 Reforming with CO_2 over Rh/Al_2O_3 and Rh/YSZ Catalysts*

1. 0.5 wt% Rh/Al_2O_3 catalyst. The isotopic experiment presented in Fig. 12 clearly indicates that the carbon-containing species which accumulate on the catalyst surface under steady-state reaction conditions originate mainly from the CO_2 molecule. Based on the transient isotopic results of this work, the following elementary reaction steps seem appropriate to describe the mechanism of CO and H_2 formation under reforming of CH_4 with CO_2:

$$CH_4(g) + s \rightarrow CH_4(s) \quad [2]$$

$$CO_2(g) + s \leftrightarrows CO_2(s) \quad [3]$$

$$CH_4(s) + (4 - x)(s) \rightarrow CH_x(s) + (4 - x)\,H(s) \quad [4]$$

$$CH_x(s) + x(s) \rightarrow C(s) + xH(s) \quad [5]$$

$$CO_2(s) + (s) \leftrightarrows CO(s) + O(s) \quad [6]$$

$$CO(s) + (s) \leftrightarrows C(s) + O(s) \quad [7]$$

$$CO(s) \leftrightarrows CO(g) + (s) \quad [8]$$

$$O(s) + H(s) \leftrightarrows OH(s) + (s) \quad [9]$$

$$OH(s) + H(s) \leftrightarrows H_2O(s) + (s) \quad [10]$$

$$H_2O(s) \leftrightarrows H_2O(g) + (s) \quad [11]$$

$$H(s) + H(s) \leftrightarrows H_2(g) + 2(s) \quad [12]$$

$$C(s) + OH(s) \leftrightarrows CO(s) + H(s). \quad [13]$$

Here (s) is a site on the rhodium surface. As already discussed in the previous section, reaction steps [2], [4], [5], the backward step [7], and the forward step [13] must be relatively fast in the case of production of CO via the CH_4 molecular pathway, as compared to the corresponding steps of CO formation via the CO_2 molecular pathway (reaction steps [3], [6], [7], and [13]). This important result may suggest that sites which accommodate carbon-containing species derived from CH_4 and CO_2 are of different nature, namely, having different reactivity towards oxygen or –OH species (a different rate constant associated with each step).

Erdöhelyi *et al.* (23) have recently investigated the CH_4 and CO_2 dissociation as well as the reforming reaction of CH_4 with CO_2 over Rh/Al_2O_3 by means of infrared and kinetic measurements. In addition to the elementary steps [2]–[13] postulated in the present work, the hydrogen-assisted dissociation of CO_2 step has been suggested (23):

$$CO_2(s) + H(s) \leftrightarrows CO(s) + OH(s). \quad [14]$$

The fact that hydrogen can enhance the rate of dissociation of CO_2 has been previously reported (24, 25). In the present work no evidence is provided that reaction step (14) cannot be considered in the sequence of steps of CO formation.

The fact that the steady-state tracing experiment with $C^{18}O_2$, similar to that given in Fig. 1, revealed no accumulated oxygen species on the catalyst surface is consistent with the view that atomic oxygen species under the present reaction conditions must be more reactive than carbon species to form gaseous CO and H_2O. This is in line with

what has been reported by other researchers (26, 27) over different reforming catalysts.

2. 0.5 wt% Rh/YSZ catalyst. The results of the steady-state tracing technique applied over the Rh/YSZ catalyst, with the goal to probe the oxygen reaction pathway from the CO_2 molecule to the various oxygen-containing product molecules, are very informative and important with respect to the mechanism of the reforming reaction of CH_4 with CO_2 over this system. The various kinds of transient isotopic experiments performed over the pure YSZ carrier (Figs. 5 and 6) clearly demonstrate that there is a large affinity for exchange of the lattice oxygen of YSZ with the oxygen atom of the CO_2 molecule at 650°C. It is known that the lattice oxygen of YSZ has a large ion mobility value, while the YSZ carrier contains a large number of oxygen vacant sites, and also other types of defect sites (5). These properties make YSZ one of the best oxygen-ion conductors (5).

The fact that no $C^{18}O$ was measured over the pure YSZ in the experiment shown in Fig. 5 strongly suggests that formation of $C^{16}O^{18}O$ and $^{16}O^{18}O$ takes place via the following elementary reaction steps:

$$^{18}O_2(g) + (2e^-/\square_s) \leftrightharpoons (^{18}O^{2-}/\square_s) + {}^{18}O_s \qquad [15]$$

$$^{18}O_s + {}^{16}O_s \leftrightharpoons {}^{16}O^{18}O \qquad [16]$$

$$C^{16}O_2(g) + {}^{18}O_s \leftrightharpoons C^{16}O^{18}O(g) + {}^{16}O_s. \qquad [17]$$

In reaction step [15], $\square_s$ is an oxygen vacancy in the lattice of YSZ, O^{2-} is a lattice oxygen species, and O_s is an atomic oxygen species at a defect site in the lattice.

The transient isotopic results shown in Figs. 3 (Rh/YSZ) and 6 (YSZ), obtained under reforming reaction conditions, demonstrate that the large pool of ^{18}O atoms formed in the YSZ support of the Rh/YSZ catalyst under the 5-min treatment of the catalyst with $CH_4/C^{18}O_2$/He mixture participates mainly in the formation of $C^{18}O$ on the Rh surface under CH_4/CO_2/He treatment, and, to a lesser extent, in the formation of $H_2{}^{18}O$ and $C^{16}O^{18}O$. Small quantities of molecular oxygen, $^{16}O^{18}O$, were also observed (Fig. 3b). Since the exchange reaction of the oxygen atom of the CO_2 molecule with the lattice oxygen of YSZ to give $C^{16}O^{18}O$ is expected to proceed also over the Rh/YSZ catalyst surface (the fraction of the Rh surface to that of YSZ is small), other reaction steps must be involved in order to explain (a) the small $C^{16}O^{18}O$ response signal obtained over the Rh/YSZ (Fig. 3b), as compared to that obtained over the YSZ alone (Fig. 6), and (b) the large response signal of $C^{18}O$ observed over the Rh/YSZ but not over the YSZ carrier. These aspects are discussed below.

Reaction steps [3], [6], and [8] are the three steps which lead to the formation of CO upon interaction of gaseous CO_2 molecule with the Rh surface of the Rh/YSZ catalyst. The possibility of CH_4 reforming with $C^{16}O^{18}O$, the latter formed over the YSZ surface by exchange of ^{18}O with CO_2 (during CH_4/CO_2/He treatment), on the Rh surface is then very likely. This route could explain both the large production of $C^{18}O$ and the small production of $C^{16}O^{18}O$ over the Rh/YSZ during steady-state tracing (Fig. 3). On the other hand, the production of $H_2{}^{18}O$ during steady-state tracing, not observed over pure YSZ, must involve ^{18}O atoms on the Rh surface. These ^{18}O atoms could arise from the dissociation of ^{18}O-labelled CO and CO_2 molecules, but also from labelled lattice oxygen species of the YSZ carrier, the former species spilled over the Rh surface or present in the periphery of Rh crystallites and the carrier surface. Production of $C^{18}O$ could take place by reaction of carbon and spilled over oxygen via reaction steps [7] and [13] described previously.

When a switch of the feed from He to the CH_4/CO_2/He mixture was performed, the production rate of CO reached a pseudosteady-state value very rapidly (in less than 5 s), indicating that the dissociation of CO_2 is a relatively fast process. Comparing the $C^{16}O^{18}O$ response obtained over the pure YSZ (Fig. 6) and that over the Rh/YSZ (Fig. 3b), and also the $C^{18}O$ response obtained over the latter catalyst (Fig. 3a), it is shown that there is an appreciable shift in the appearance of the peak maximum in the rate of production of $C^{16}O^{18}O$ and $C^{18}O$ (no $C^{18}O$ was observed over the pure YSZ). These results may mean that the oxygen spillover process over the Rh/YSZ catalyst, as discussed in the previous paragraph, may contribute to the observed response shifts. The extent of contribution of each of these processes cannot of course be deduced from the present experiments. On the other hand, the oxygen spillover process must have a limited extent with time on stream, unless there is a source of oxygen supply to the oxygen vacancies created. Such a source could be the CO_2 by its dissociation onto the YSZ support. However, the latter process was not observed at $T = 650$°C in the present work. At higher temperatures, this process could take place.

The steady-state tracing experiment with labelled $^{13}CH_4$ or $^{13}CO_2$ (Fig. 2) resulted in a non-measurable quantity ($\theta_c < 0.02$) of active carbon-containing species which participate in the formation of CO during catalysis. This result is consistent with the H_2 TPH result reported in Part 1 (1), which revealed an amount of total carbon formed equivalent to θ_c of 0.03 after 2 h of reforming reaction. On the other hand, over the Rh/Al_2O_3 catalyst there exists on the Rh surface an amount of active carbon-containing species equivalent to θ_c of 0.2, originating from the CO_2 molecule (Figs. 1 and 12). In Part 1 (1) it is illustrated that the initial TOF of CO formation over the Rh/YSZ catalyst is more than twice higher than that obtained over the Rh/Al_2O_3 catalyst. Given the evidence provided in Part 1 (1) that the present reaction system might inherently be con-

sidered as structure insensitive, the difference in initial activity observed over the present two catalysts (having a different mean Rh particle size) must be explained based on other reasons.

It is clear from the mechanistic steps [4], [5], [7], and [13] of the reforming reaction of CH_4 with CO_2 given previously that formation of CO from CH_4 requires the oxygen atom of the CO_2 molecule. As is illustrated in this work, and extensively discussed in previous paragraphs, the lattice oxygen of YSZ may participate in reaction steps leading to CO formation on the Rh surface at $T > 650$°C. It might then be reasonable to suggest that the activity of such oxygen species may be higher than that of oxygen species derived from the dissociation of CO_2 (step [6]) and CO (step [7]), leading, therefore, to an enhancement in the rate of CO formation, via reaction steps [7], [9], and [13], when Rh is supported on YSZ than on Al_2O_3.

It has been reported (15) that under differential conditions there exists some moderate deactivation of the Rh/YSZ catalyst. On the other hand, the amount of carbon formed over this catalyst is very small (1), and alterations of Rh particle size during reforming reaction are also small (1). From these results it is speculated whether some poisoning of specific Rh sites by strongly bound oxygen atoms, the latter originating from the lattice of YSZ carrier, occurs, contributing to the catalyst deactivation observed. Further discussion on the aspect of catalyst deactivation was given in Part 1 (1).

CONCLUSIONS

The following conclusions are derived from the results of the present work.

1. The quantity of active carbon-containing intermediate species which lead to the formation of CO during reforming reaction of CH_4 with CO_2 over the Rh/Al_2O_3 catalyst at 650°C is equivalent to a surface coverage of 0.2. These active carbon species, which consist of both adsorbed CO and atomic carbon, are found in the reaction route of the CO_2 molecule, while the corresponding amount of active carbon-containing species derived from the reaction route of CH_4 molecule is very small ($\theta_c < 0.02$). On the other hand, the reforming reaction over the Rh/YSZ catalyst results in very small amounts of active carbon-containing species derived either from the CH_4 or the CO_2 molecular reaction route ($\theta_c < 0.02$).

2. The surface coverage of active oxygen species which lead to the formation of CO during the reforming reaction over the Rh/Al_2O_3 catalyst at 650°C is found to be very small ($\theta_c < 0.02$). However, there is a large pool of lattice oxygen species of the yttria-stabilized zirconia (YSZ) support which participate in the formation of CO during the reforming reaction at 650°C over the Rh/YSZ catalyst. Steady-state tracing results suggest that part of this lattice oxygen may migrate onto the Rh surface to form CO, while a large part of it exchanges with gaseous CO_2 followed by dissociation to CO and atomic oxygen on the Rh surface. Such lattice oxygen species might be considered responsible for the higher TOF values obtained over the Rh/YSZ as compared to the Rh/Al_2O_3 catalyst.

3. The present steady-state tracing results obtained over the Rh/Al_2O_3 catalyst suggest that reaction steps of the CH_4 molecular reaction pathway to form CO are faster than those of the CO_2 molecular reaction pathway.

ACKNOWLEDGMENT

Financial support by the Commission of the European Community (Contrast JOU2-CT92-0073) is gratefully acknowledged.

REFERENCES

1. Zhang, Z. L. Tsipouriari, V., Efstathiou, A. M., and Verykios, X. E., *J. Catal.* **158,** 51 (1996).
2. Efstathiou, A. M., Papageorgiou, D., and Verykios, X. E., *J. Catal.* **141,** 612 (1993).
3. Stockwell, D. M., Chung, J. S., and Bennett, C. O., *J. Catal.* **110,** 354 (1988).
4. Efstathiou, A. M., Ph.D. thesis, University of Connecticut, 1989.
5. Vayenas, C. G., Bebelis, S., Yentekakis, I. V., and Lintz, H.-G., *Catal. Today* **11,** 303 (1992).
6. Tanaka, Y., Iizuka T., and Tanabe, K., *J. Chem. Soc. Faraday Trans. 1* **78,** 2215 (1982).
7. Yates, J. T., Duncan, T. M., Worley, S. D., and Vaughan, R. W., *J. Chem. Phys.* **70,** 1219 (1979).
8. Worley, S. D., Rice, C. A., Mattson, G. A., Curtis, C. W., Guin, J. A., and Tarrer, A. R., *J. Chem. Phys.* **76,** 20 (1982).
9. Solymosi, F., Bansagi, T., and Erdöhelyi, A., *J. Catal.* **72,** 166 (1981).
10. Edwards, J. F., and Schrader, G. L., *J. Phys. Chem.* **88,** 5620 (1984).
11. Dalla Betta, R. A., and Shelef, M., *J. Catal.* **48,** 111 (1977).
12. Little, L. H., "IR Spectra of Adsorbed Species," p. 47. Academic Press, New York, 1966.
13. Solymosi, F., Tombacz, I., and Kocsis, M., *J. Catal.* **75,** 78 (1982); Solymosi, F., and Erdöhelyi A., *J. Catal.* **91,** 327 (1985).
14. (a) Biloen, P., *J. Mol. Catal.* **21,** 17 (1983); (b) Yang, C.-H., Soong, Y., and Biloen, P., *in* "Proceedings 8th International Congress on Catalysis, Berlin, 1984," Vol. II, p. 3. Verlag-Chemie, Weinheim, 1984.
15. Tsipouriari, V., Efstathiou, A. M., Zhang, Z. L., and Verykios, X. E., *Catal. Today* **21,** 579 (1994).
16. Solymosi, F., Erdöhelyi, A., and Kocsis, M., *J. Catal.* **65,** 428 (1980).
17. Efstathiou, A. M., and Bennett, C. O., *J. Catal.* **120,** 118 (1989).
18. Efstathiou, A. M., and Bennett, C. O., *J. Catal.* **120,** 137 (1989).
19. Pino, P., Piacenti, F., and Bianchi, M., *in* "Organic Synthesis via Metal Carbonyls" (I. Wender and P. Pino, Eds.), Vol. 2, p. 43. Wiley, New York, 1977.
20. Chuang, S. S. C., and Pien, S. I., *J. Catal.* **135,** 618 (1992).
21. Efstathiou, A. M., Chafik, T., Bianchi, D., and Bennett, C. O., *J. Catal.* **147,** 24 (1994).
22. Efstathiou, A. M., Chafik, T., Bianchi, D., and Bennett, C. O., *J. Catal.* **148,** 224 (1994).
23. Erdöhelyi, A., Cserényi, J., and Solymosi, F., *J. Catal.* **141,** 287 (1993).
24. Solymosi, F., Erdöhelyi, A., and Kocsis, M., *J. Catal.* **65,** 428 (1980).
25. Hendersen, M. A., and Worley, S. D., *J. Phys. Chem.* **89,** 392 (1985).
26. Winkler, A., Guo, X., Siddiqui, P. L., Hagans, P. L., and Yates, J. T., Jr., *Surf. Sci.* **201,** 419 (1988).
27. Hickman, D. A., Haupfear, E. A., and Schmidt, L. D., *Catal. Lett.* **17,** 223 (1993).